Biochemical and Biophysical Research Communications **257,** 239–243 (1999)
Article ID bbrc.1999.0440, available online at http://www.idealibrary.com on IDEAL®

Synergistic Inhibition of Carboxypeptidase A by Zinc Ion and Imidazole

William L. Mock[1] and Lingyan Wang
Department of Chemistry, University of Illinois at Chicago, Chicago, Illinois 60607-7061

Received February 8, 1999

Zinc ion in solution yields a 560-fold enhancement in the kinetic inhibition of carboxypeptidase A by the simple heterocycle imidazole, behavior attributed to formation of a ternary complex of the three species. However, the effect is partially negated by formation of less-inhibitory $Zn^{2+}(C_3H_4N_2)_{2-4}$ coordination complexes, providing for the enzyme an anomalous profile of catalytic rate versus imidazole concentration. © 1999 Academic Press

The well-studied prototype of the metalloproteases, carboxypeptidase A, exhibits many puzzling kinetic features. Among these are various phenomena of substrate-selective stimulation or retardation of catalysis rate by exogenous agents (1-7). Because the chemical-catalytic mechanism of this zinc enzyme remains incompletely resolved (8), elucidation of such behavior could potentially reveal mechanistic detail. Several years ago an observation was made that the presence in solution of the simple metal-liganding heterocycle imidazole ($C_3H_4N_2$) *activated* a particular preparation of carboxy-peptidase A catalytically (9). We have undertaken a further kinetic study, for benefit of any mechanistic insight that this phenomenon might provide.

MATERIALS AND METHODS

Enzyme and buffers. Bovine pancreatic carboxypeptidase A (ZnCpA,[2] EC 3.4.17.1) was obtained from Sigma Chemical Co. (No. C 0386). It was recrystallized by dialysis according to established procedures before use (10). Enzyme concentrations were estimated using $\epsilon_{278} = 6.42 \times 10^4\ M^{-1}\ cm^{-1}$. Buffers employed in this work for kinetic analysis were (0.05 M each) as follows: 2-(*N*-morpholino)ethanesulfonic acid, pH of 5.5-7.0; tris-*N*-(hydroxymethyl)aminomethane, pH of 7.5-8.5; 2-amino-2-methyl-1,3-propanediol, pH of 9.0-10.0. All enzyme work was done with solutions 1.0 M in sodium chloride.

Substrate and enzyme ligands. Kinetic assays for inhibition routinely employed the convenient substrate anisylazoformyl-L-phenylalanine (11), reported $k_{cat}/K_m = 4.1 \times 10^5\ M^{-1}\ s^{-1}$ at pH 7.7. The portrayed kinetic behavior with imidazoles is not unique to this substrate; a similar pattern was noted with a peptide substrate (furanacryloylphenylalanylphenylalanine) as well as with an ester substrate (chlorocinnamoylphenyllactic acid). Imidazole and *N*-methylimidazole were commercial materials, purified by recrystallization or distillation before use.

Kinetic analysis. Velocity measurements for catalytic hydrolysis of the substrate were carried out at 25.0 (±0.1) °C in buffers previously listed, with spectrophotometric (350 nm, 2 cm pathlength) analysis and the method of initial rates. Stock solutions of the arylazoformylamide substrate were shielded from light to avoid *cis-trans* isomerization of the azo linkage. Concentration of enzyme in assays was maintained well below substrate concentration for kinetic parameter determinations in all cases, and substrate concentration was well below K_m for competitive K_i measurements. Because this investigation was concerned exclusively with competitive binding phenomena, relative rates have been normalized (Figures). The limiting kinetic parameters were obtained by a nonlinear least-squares fit of data to appropriate equations, $(v)_{apparent} = (v)_{lim}/(1 + [I]/K_i)$ in the case of simple competitive inhibition, or alternatively as given in the Figure legend. All pH values in this article are calibrated pH meter readings uncorrected for ionic strength effects. Tolerances listed are standard errors from least-squares analysis.

RESULTS

Inhibition and re-activation. A conspicuous irregularity characterizes the catalytic behavior of carboxypeptidase A in the presence of imidazole. Because of the affinity of imidazole for metal ions in solution, initial investigations of its kinetic influence on the enzyme were conducted with extra Zn^{2+} present. Zinc was incorporated in order to suppress any potential stripping of the essential metal ion from the enzyme active site by the added ligand. Although Zn^{2+} in the μM-mM concentration range is known to be inhibitory by itself as regards carboxypeptidase A (12, 13), concurrent formation of zinc-imidazole coordination complexes should exert a buffering action diminishing the actual concentration of free metal ion. Figure 1 shows the anomalous but reproducible variation (which is independent of substrate type) seen to occur in the specificity constant k_{cat}/K_m in the presence of increasing amounts of imidazole. The peculiar pattern of be-

[1] To whom correspondence should be addressed. Fax: 312 996-0431. E-mail: wlmock@uic.edu.

Abbreviations: ZnCpA, catalytically active carboxypeptidase A (with the normal 1 equivalent of zinc ion ligated at the active site); Im, imidazole ($C_3H_4N_2$).

0006-291X/99 $30.00

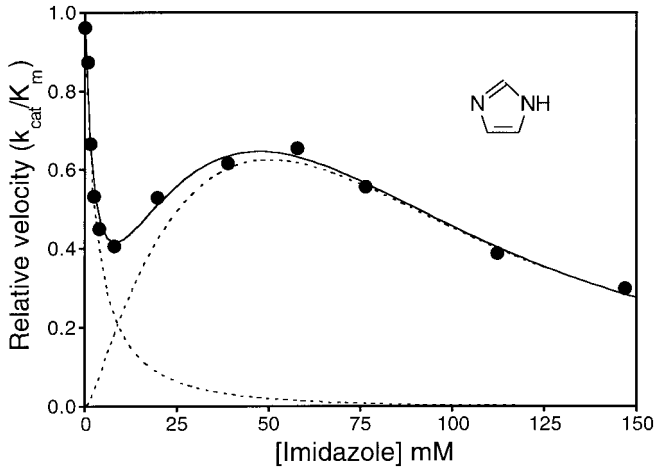

FIG. 1. Normalized velocity of catalysis (k_{cat}/K_m) by carboxypeptidase A as a function of imidazole concentration, in presence of 0.1 mM Zn^{2+}. Assay substrate was anisylazoformylphenyl-alanine, 0.01 mM ($\ll K_m$, 0.11 mM) (11), in buffered saline solution, pH 8. Empirical curve assumes that one imidazole binds and negates catalytic activity (phase 1), a second binds and restores activity (phase 2), and additional imidazoles enter and again extinguish activity (phase 3). Dashed lines deconvolute first and second phases.

havior exhibited, namely, an initial inhibition followed by re-activation and then by a subsequent further downturn in activity, was not immediately explicable. One $C_3H_4N_2$ ligand seems to bind initially in the sub-mM concentration range, with loss of enzymic activity. This phase of the profile was shown to be competitive in nature (k_{cat}/K_m for the substrate was perturbed, but evidently not k_{cat}). However, it could not be determined for certain whether such inhibition was partial or complete, because at somewhat higher concentrations a second imidazole apparently interacts with the initial enzyme complex, reversing the effect of the first ligand (re-activation). This seeming behavior is modelled in its simplest form by the dashed lines in Fig. 1. The eventual flagging of catalytic activity with yet greater amounts of imidazole (>0.1 M) requires no special rationalization. A measure of imidazole-induced demetalation of the enzyme, or some interference with proper protein folding due to the added heterocycle might be expected in this higher concentration range. But, the catalytic re-activation expressed within the second phase of the curve in Fig. 1 (with concentration of $C_3H_4N_2 \sim 25$ mM) seemed mechanistically significant, and it called for further investigation.

Protonation. Similar behavior was exhibited by *N*-methylimidazole, with a less-pronounced re-activation, but no comparable effect was seen with *N,N′*-dimethylimidazolium ion (neither significant inhibition nor activation). Consequently, the unprotonated and neutral species ($C_3H_4N_2$ rather than $C_3H_4N_2 \cdot H^+$) was surmised to be responsible in the case of imidazole. This was borne out by an examination of pH dependence of K_i, with respect to the initial inhibitory phase, in the case of *N*-methylimidazole. As shown in Fig. 2, binding of heterocycle to carboxypeptidase A seems to fall off markedly on the acidic limb of the pH profile (solid symbols denote apparent pK_i values), particularly so for hydronium ion concentrations below the known pK_a of 7.2 for *N*-methyl-imidazolium ion in saline solution (14). However, adjustment for protonation of the inhibitor yields the upper profile (open circles represent corrected pK_i values, excluding the cation). The resulting curve shows only a feeble pH dependence, at best. The simplest explanation is that the catalytic effect within this inhibitory phase is entirely due to unprotonated imidazole. The re-activation phase persisted at higher pH, but could not be examined on the acidic limb of the profile.

Synergism. An ultimate resolution of the inhibition and re-activation kinetic phenomenon only became apparent when the influence of concurrent variation within the concentrations of both imidazole and zinc ion was investigated. Figure 3 provides a graphic illustration of the catalytic kinetic consequences from simultaneously co-varying the amount of each of these species available to the enzyme. As has been previously reported, Zn^{2+} alone is a competitive inhibitor for carboxypeptidase A. The value of the inhibition constant that we find, K_{Zn} 30 ± 3 μM at pH 7.8 (curve depicted on left rear wall of Fig. 3), agrees with previous findings, $K_i \sim 15$ μM (12). On the other hand, imidazole by itself only weakly inhibits carboxypeptidase A, K_{Im} 82 ± 13 mM at pH 7.8 (right rear wall of Fig. 3, extrapolated value). However, the presence of relatively low concentrations of Zn^{2+} (1-10 μM) greatly enhances the inhibition by imidazole. This effect may

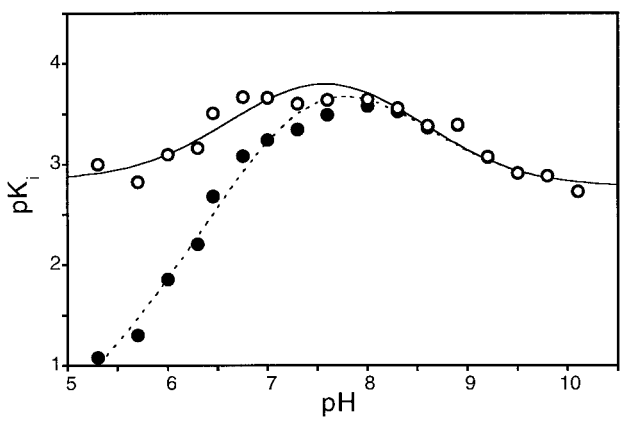

FIG. 2. Dependence upon pH for apparent value of pK_i ($-\log K_i$) for *N*-methylimidazole and carboxypeptidase A, in presence of 0.1 mM Zn^{2+}. Filled symbols correspond to uncorrected inhibition by $[(Me)Im]_t$ (i.e., both methylimidazole plus methylimidazolium ion). Open circles correspond to inhibition resulting from unprotonated methylimidazole only. Empirical curve for latter symbols (solid line) assumes slightly tighter binding at intermediate pH, although a straight horizontal line might be equally acceptable (see Discussion).

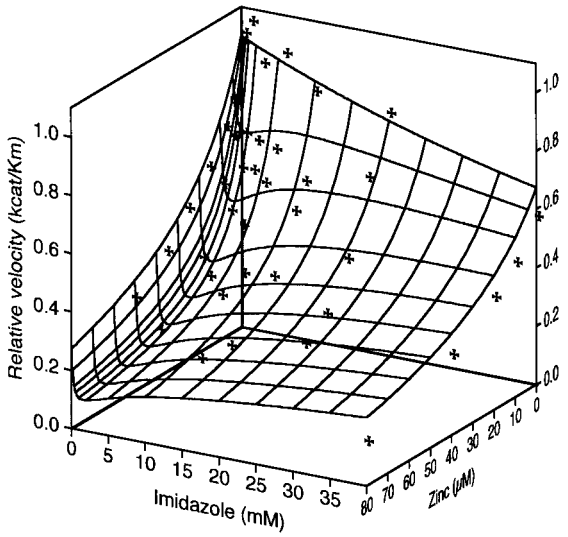

FIG. 3. Catalytic consequences (k_{cat}/K_m) of simultaneous variation in concentration of both Zn^{2+} and imidazole with carboxypeptidase A. Grid lines correspond to least-squares global fit for following equation (from Scheme 1 mechanism): $(v)_{apparent} = (v)_{lim}/\{1 + [Im]_t/K_{Im} + (1 + ([Im]_t/\alpha K_{Im}) \cdot (1 + [Im]_t/\alpha' K_{Im} + ([Im]_t/\alpha' K_{Im})^2)) \cdot ([Zn]_t/K_{Zn})/(1 + [Im]_t/K_1 + [Im]_t^2/K_2 + [Im]_t^3/K_3 + [Im]_t^4/K_4)\}$. Parameters: $(v)_{lim}$ 1.00 ± 0.02 (normalized), K_{Im} 82 ± 13 mM, K_{Zn} 30 ± 3 μM, α 0.0018 ± 0.0004, α' 0.11 ± 0.02, K_1-K_4 literature values (see Discussion). Cross marks symbolize data points, which have a standard deviation of 8% (relative velocity) with respect to the fitted surface.

be seen within the grid depicted in Fig. 3, in the form of a valley near the left rear wall. The steep declination in the grid lines passing into that crease in the projected surface (correlating with increasing concentration of $C_3H_4N_2$) indicates a strong *synergistic* effect: A low concentration of zinc ion greatly enhances the potency of imidazole in its inhibition of carboxypeptidase A. However, this is a transitory phenomenon. Yet more imidazole relaxes the inhibitor expression (velocities ascending from the valley), as was previously depicted in Fig. 1 for nearly saturating amounts of Zn^{2+}. A probable explanation for this pattern follows.

DISCUSSION

Quantification. The variation in the specificity constant k_{cat}/K_m depicted in Fig. 3 suggests a synergistic inhibition phenomenon, involving zinc ion and imidazole. It has been known for some time that excess Zn^{2+} in solution inhibits carboxypeptidase A (12, 13). A crystal structure of the Zn-inhibited enzyme has been presented (15, 16). That foreknowledge supplies an interpretive point of departure. For brevity in analyzing the synergism, some shorthand notations will henceforth be employed: "Im" for imidazole, "Zn" for zinc ion, and "ZnCpA" for native carboxypeptidase A (catalytically functional, with a single active-site zinc ion). It now appears that the ternary complex ZnCpA · Zn · Im is considerably more favored thermodynamically than either of the binary complexes ZnCpA · Zn or ZnCpA · Im. Expressed equivalently, ligand Im binds to ZnCpA · Zn some 560-fold more tightly than to ZnCpA itself, according to a numerical analysis subsequently to be presented. However, it is well known that the ligands imidazole and zinc ion by themselves also form a series of coordination complexes: Zn · Im, Zn · Im_2, Zn · Im_3, and Zn · Im_4 (17). From the quantitative interpretation which ensues, a conclusion follows that Zn · Im inhibits by anomalously firm binding to ZnCpA as just suggested (behavior indistinguishable from tight ligation of imidazole to ZnCpA · Zn), but that the higher complexes Zn · Im_2, Zn · Im_3, and Zn · Im_4 are much less inhibitory, so that as Zn · Im becomes depleted at higher imidazole concentrations due to Zn · $Im_{2\text{-}4}$ formation, an effective re-activation of the enzyme occurs in consequence. Such a formulation offers the simplest explanation for the pattern of kinetic behavior exhibited in the previous Figures.

Justification of that interpretation comes from the surface depicted by the grid in Fig. 3, which corresponds to a nonlinear least-squares fit of relative velocity data to an equation derived for Scheme 1. Values for the binary dissociation constants as previously given, for zinc (K_{Zn}) and imidazole (K_{Im}), are readily ascertained from the corresponding limiting hyperbolic inhibition profiles, as determined individually for the respective ligands (rear walls of Fig. 3). To quantify the inhibitory synergism shown by these species jointly, it was necessary to limit the number of adjustable parameters. Consequently, the concentrations of the various zinc-imidazole species [Zn · Im_n] in solution were independently set during the surface-fitting exercise, from known binding constants (17). This is permissible since the concentration relationship among the kinetically pertinent species is $[Im]_t \gg [Zn]_t \geq [ZnCpA]_t$ for all relevant ternary points on the grid of Fig. 3 (i.e., any ligation involving the enzyme does not seriously deplete the total amount of Zn and Im available). The following dissociation constants were used in assigning concentrations for complexes [Zn · Im_n]: K_1 0.753 mM, K_2 2.286 $(mM)^2$, K_3 21.88 $(mM)^3$, K_4 912 $(mM)^4$, as defined in Scheme 1. These numbers had been previously secured for solutions 3 M in potassium chloride (17), but they should be sufficiently accurate to employ in conjunction with our kinetic data obtained in 1 M sodium chloride (the counter-ion dependence of Zn^{2+}-ligation by Im was shown to be slight). Upon inserting these constants as nonadjustable parameters in the appropriate equation as given in the legend to Fig. 3, the desired quantification of inhibitory synergism may be obtained, by a multidimensional least-squares fit of velocity data to that formula. The purpose of the exercise is to secure the coefficient designated in Scheme 1 as α, which relates the dissociation constants for the ternary enzyme complex (ZnCpA · Zn · Im) to that for binary complexes (ZnCpA · Zn or ZnCpA · Im). In the

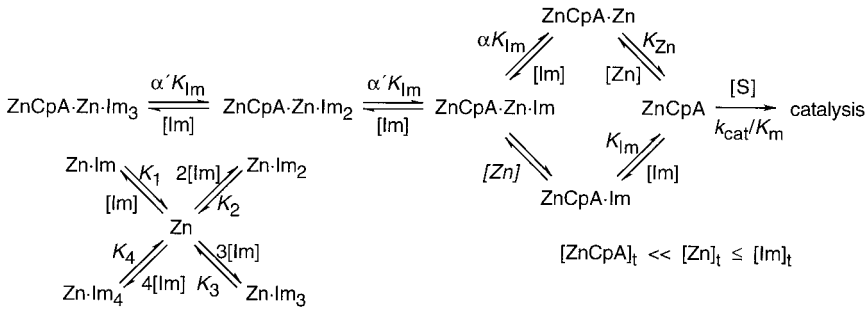

SCHEME 1

present instance its fitted value of 0.0018 ± 0.0004 indicates just how much more tightly imidazole attaches to the binary complex ZnCpA · Zn than to the catalytically active form of the enzyme ZnCpA; i.e, upon ligation of a second zinc ion to the enzyme, the apparent dissociation constant for imidazole and the enzyme drops from a value of 83 mM to a value of 0.15 mM (αK_{Im}), a factor of 560-fold. Logically, however, and in order to satisfactorily accommodate all of the data in Fig. 3, it was necessary to assume that additional inhibitory enzyme complexes of stoichiometry ZnCpA · Zn · Im_2 and ZnCpA · Zn · Im_3 also form, albeit representing relatively weaker incremental imidazole affinity than seen within the ternary species ZnCpA · Zn · Im. It was not possible to separate analytically the affinities of these two higher-order adducts, and so they are accommodated with a mutually applicable second coefficient, designated α' (mean value), which is allowed to apply to both ZnCpA · Zn · Im_2 and ZnCpA · Zn · Im_3 (Scheme 1). The additional coefficient has a fitted magnitude of only 0.11 ± 0.02, indicating that second and third imidazoles each bind about 60-fold less tightly to ZnCpA · Zn · Im, versus the prefatory association between imidazole and ZnCpA · Zn giving ZnCpA · Zn · Im. In summary, the valley in the surface depicted in Fig. 3 arises from an exceptional affinity of Zn · Im for the enzyme. However, with increasing imidazole concentrations that species becomes depleted relative to higher-order complexes Zn · Im_n, which are considerably less inhibitory, so that the enzyme appears to re-activate.

The pH profile for inhibitor binding (Fig. 2), determined for carboxypeptidase A with *N*-methyl-imidazole, merits brief comment. To a first approximation, pK_i appears independent of pH after correction for inhibitor protonation, with perhaps a slightly higher affinity of the heterocycle for the enzyme near neutrality. The pattern suggests that binding has been perturbed only marginally by enzymic ionizations. However, this data was collected with excess zinc ion present (0.1 mM). Because zinc inhibition by itself manifests a strong pH dependence (pH 6.5, $K_i \approx 0.25$ mM; pH 7.5, $K_i \approx 0.0025$ mM; pH 8.5, $K_i \approx 0.0025$ mM) (12), the exhibited profile probably subsumes both binary (K_{Im}) and ternary (αK_{Im}) complexes, according to pH. It does not seem feasible to separate them analytically, with such little variation in apparent pK_i. Furthermore, the extreme acidic limb of the profile may also reflect some enzyme degradation, as suggested by Fig. 1 for relatively high imidazole concentration. Consequently, no additional interpretation will be provided.

Conclusion. A reason for the much greater affinity of imidazole toward ZnCpA · Zn than toward the native enzyme ZnCpA by itself is difficult to surmise. It seems likely that the tightly-bound imidazole ligates to the extrinsic (added) metal ion, rather than to the catalytic (intrinsic) zinc ion. According to previous crystallographic evidence (15, 16), the extrinsic zinc ion enters the active site of ZnCpA and links the hydroxide ligand of the catalytic zinc in the native enzyme (18-20) with the side-chain carboxylate of enzymic residue Glu 270. The pH dependence of Zn^{2+} binding, which indicates a concurrent loss of a proton, is consistent with formation of such an (enzyme-ligand)$_3$Zn—O—Zn—O_2C(Glu) bridge (12). Within the published structures of that ZnCpA · Zn complex there does not appear to be an incipient ligation position available on the catalytic zinc ion, but the extrinsic zinc ion retains solvent and/or halide species within its coordination sphere, which could become displaced by imidazole. It might alternatively be imagined that an imidazolate ring inserts between the catalytic and extrinsic Zn ions (with a ring-nitrogen coordinated to each, replacing the oxide bridge), but *N*-methylimidazole seems to show the same synergistic binding phenomenon, which disfavors such an explanation.

Finally we note that, on account of thermodynamic reciprocity, saturating amounts of imidazole must also enhance binding of zinc ion to ZnCpA, and by the same factor α. In other words, the dissociation constant K_{Zn} becomes diminished to an apparent value of ~50 nM (αK_{Zn} at pH 7.8) in the presence of excess $C_3H_4N_2$. This could be of practical significance, for if an imidazole analogue or derivative could be found with favorable enzymic specificity arising from an intrinsic affinity for the non-zinc portion of the active site of ZnCpA, it might usefully induce metal-ion inhibition of the en-

zyme by exploiting prevalent physiological concentrations of Zn^{2+}, a stratagem recently advanced ably for the serine proteases (21). This would represent a new approach to metalloprotease inactivation, and one which harbors potential for general applicability.

ACKNOWLEDGMENT

This work was supported by NIH Grant GM39740.

REFERENCES

1. Coleman, J. E., Pulido, P., and Vallee, B. L. (1966) *Biochemistry* **5,** 2019–2025.
2. Davies, R. C., Auld, D. S., and Vallee, B. L. (1968) *Biochem. Biophys. Res. Commun.* **31,** 628–633.
3. Davies, R. C., Riordan, J. F., Auld, D. S., and Vallee, B. L. (1968) *Biochemistry* **7,** 1090–1099.
4. Glovsky, J., Hall, P. L., and Kaiser, E. T. (1972) *Biochem. Biophys. Res. Commun.* **47,** 244–247.
5. Bunting, J. W., and Myers, C. D. (1975) *Can J. Chem.* **53,** 1993–2004.
6. Sebastian, J. F., and Lo, W.-Y. (1978) *Can. J. Biochem.* **56,** 329–333.
7. Sebastian, J. F., Hinks, R. F., and Reuland, R. V. (1987) *Biochem. Cell. Biol.* **65,** 717–725.
8. Mock, W. L. (1998) *in* Comprehensive Biological Catalysis (Sinnott, M., Ed.), Vol. 2, Chap. 11, pp. 425–453, Academic Press, UK.
9. Bodwell, J. E., and Meyer, W. L. (1981) *Biochemistry* **20,** 2767–2777.
10. Mock, W. L., and Chen, J.-T. (1980) *Arch. Biochem. Biophys.* **203,** 542–552.
11. Mock, W. L., Liu, Y., and Stanford, D. J. (1996) *Anal. Biochem.* **239,** 218–222.
12. Larsen, K. S., and Auld, D. S. (1989) *Biochemistry* **28,** 9620–9625.
13. Larsen, K. S., and Auld, D. S. (1991) *Biochemistry* **30,** 2613–2618.
14. Jencks, W. P., and Gilchrist, M. (1968) *J. Amer. Chem. Soc.* **90,** 2622–2637.
15. Gomez-Ortiz, M., Gomis-Rüth, F. X., Huber, R., and Avilés, F. X. (1997) *FEBS Letters* **400,** 336–340.
16. Bukrinsky, J. T., Bjerrum, M. J., and Kadziola, A. (1998) *Biochemistry* **37,** 16555–16564.
17. Forsling, W. (1977) *Acta Chem. Scand.* **A31,** 759–766.
18. Mock, W. L., and Tsay, J.-T. (1986) *Biochemistry* **25,** 2920–2927.
19. Mock, W. L., and Tsay, J.-T. (1988) *J. Biol. Chem.* **263,** 8635–8641.
20. Mock, W. L., Freeman, D. J., and Aksamawati, M. (1993) *Biochem. J.* **289,** 185–193.
21. Katz, B. A., Clark, J. M., Finer-Moore, J. S., Jenkins, T. E., Johnson, C. R., Ross, M. J., Luong, C., Moore, W. R., and Stroud, R. M. (1998) *Nature (London)* **391,** 608–612.